applied optics

Multi-spectral infrared spectroscopy for robust plastic identification

Abraham Vázquez-Guardado,[1,2] Mason Money,[3] Nathaniel McKinney,[3] and Debashis Chanda[1,2,3,4,*]

[1]CREOL, College of Optics and Photonics, University of Central Florida, Orlando, Florida 32816, USA
[2]NanoScience Technology Center, University of Central Florida, Orlando, Florida 32826, USA
[3]Department of Electrical Engineering and Computer Science, University of Central Florida, Orlando, Florida 32816, USA
[4]Department of Physics, University of Central Florida, Orlando, Florida 32816, USA
*Corresponding author: debashis.chanda@creol.ucf.edu

Received 21 April 2015; revised 21 June 2015; accepted 24 June 2015; posted 25 June 2015 (Doc. ID 238391); published 18 August 2015

The identification and classification of plastics plays an important role in waste management and recycling processes. Present electrical and optical sorting techniques lack the required resolution for accurate identification in a high throughput manner for a diverse set of plastics commonly found in municipal waste. In this work a multi-spectral infrared spectroscopic technique is employed to construct a unique fingerprint library of 12 plastic resin groups that are commonly encountered in municipal waste. We test the proposed method in a blind plastic identification experiment, which shows excellent unbiased identification accuracy. This simple optical technique in combination with the multi-spectral library will enable high throughput and accurate detection of various plastics from recovered solid waste.

OCIS codes: (300.6340) Spectroscopy, infrared; (160.5470) Polymers; (120.5700) Reflection; (300.6170) Spectra.

http://dx.doi.org/10.1364/AO.54.007396

1. INTRODUCTION

Waste management for recycling is one of the most important needed tasks in order to save the world from the immense quantity of solid waste being disposed every day [1]. In 2012, approximately 251 million tons of solid waste was generated in the USA alone, where 13% of it was different kinds of plastics. However, out of the 87 million tons of recovered solid waste only a total of 3% corresponded to plastics, and the remaining was damped into landfills, making plastic one of the major environmental pollutants [2]. Hence, a large-scale effort is still needed in order to increase the plastic recycling outcome. In the polymer recycling industry, resin identification is the most important step in order to guarantee the economical worthiness of the process since cross contamination of incompatible resins can degrade the quality of the entire recycled batch. Moreover, this task becomes extremely challenging due to the large diversity of plastics present in the recovered plastic stocks from municipal waste, which mandates accurate classification before entering the recycling chain [3,4]. To identify and sort different families of plastics, techniques such as triboeletrostatic separation based on the electrostatic charge of a known plastic mixture [5–7], magnetic density [8,9], air flotation [10], automated image analysis systems to discriminate plastic bottles of a specific plastic resin [11], and some combination of these [12,13] have been developed. These methods use prior knowledge of the material's physical properties for external stimulus-based detection. Likewise, all of these methods work well in a known material stock but fail in a realistic scenario of blind identification of an unknown combination of plastics.

In order to tackle this crucial step in the recycling chain, accurate identification of plastics based on chemical composition is very important, as pointed out earlier. For this purpose various methods such as Fourier transform infrared (FTIR) spectroscopy [14,15], Raman spectroscopy [16], direct chemical element identification based on laser-induced breakdown spectroscopy [17,18], and hyperspectral imaging methods [8,19,20] have been studied. These methods have proven to be reliable in identifying unique molecular vibrational fingerprints in polymer compounds [21], especially near-infrared (NIR) FTIR spectroscopy for its robustness and flexibility. FTIR spectroscopy techniques vary between different configurations such as transmission, absorption, or reflection, which is restricted by the application needs or the sample preparation method, but the underlying physics involved in the detection remain the same. In fact, by measuring reflectance spectra one can straightforwardly estimate the absorption coefficients by performing the Kramers–Kronig transformation [21–23]. The spectral domain is dictated by the dominant vibrational modes present in those spectral bands. However, unique identification is challenging due to the weaker spectral features that are further overlapped in frequency among various plastics due to similar vibrational mode overtones generated by the main

Table 1. List of 12 Analyzed Plastic Resin Families Analyzed, Their Resin Identification Code, and Their Common Usage[a]

	Plastic		RIC	Typical Usage
Group 1	PET	Polyethylene Terephthalate	1	Drinking water and soda bottles, fruit containers
	HDPE	High Density Polyethylene	2	Container caps, water bottle caps, toys, household utensils
	PVC	Polyvinyl Chloride	3	Packaging containers, pipes, electrical cable insulators
	LDPE	Low Density Polyethylene	4	Laboratory wash bottles, consumer bags
	PP	Polypropylene	5	Kitchen containers, milk containers
	PS	Polystyrene	6	Disposable tape dispensers, compact disc cases, egg packing
	PC	Polycarbonate	7	Dielectric high-stability capacitors, compact discs, laboratory safety goggles
Group 2	Acrylic	Acrylic	7	Lens for glasses, windows (skylights), LCD screens
	Nylon	Polyamide	7	Clothing, thermoplastic, luggage, parachutes, backpacks
	POM	Polyoxymethylene (Acetal)		Small gear wheels, seat-belt components, ball bearings
	ABS	Acrylonitrile Butadiene Styrene		Lego bricks, musical instruments, protective headgear
	PTFE	Polytetrafluoroethylene		Dielectric layers, seals, gaskets, fittings

[a]Group 1, commonly used plastics; group 2, specialized plastics.

functional groups. Vibrational mode overtones of the functional groups, mainly XH, XH_2, and XH_3 (X = C, N, O, etc.), tend to be weaker in the NIR, but their fundamental modes are stronger in the mid-infrared (MIR) domain. In addition, some resonances are only present in the MIR domain for some polymers, rendering the NIR domain useless.

In this work a multi-spectral detection technique that covers both the NIR (1.5–2.0 μm) and the MIR (3–12 μm) spectral domains is developed to capture unique vibrational overtones of commonly used as well as specialized plastics. Several multi-spectral reflectance features are statistically identified to create a unique combination of spectral features (unique spectral fingerprint). Apart from spectral features, an additional degree of freedom is added by distinguishing them by either valleys (v) or peaks (p) associated with their vibrational resonance modes. The reported multi-spectral and multi-dimensional fingerprint library can be used to identify almost all widely used plastic resin groups with almost 100% accuracy for the first time, to the best of our knowledge.

2. MATERIALS AND METHODS

A broad spectrum of plastics was collected in order to cover the diversified plastic items widely encountered in the municipal waste: 12 plastic resins were chosen and divided in two groups. The most common plastics are generated mainly from household and end consumer products and are grouped into group 1, labeled by the society of the plastic industry with a resin identification code (RIC). This group includes PET, HDPE, PVC, LDPE, PP, PS, and PC. In the collected samples PS is found in two phases, foam (PS-f) and solid (PS-s), which showed clear distinction in the reflectance spectra. Another group of plastics are those that are encountered in more specialized applications but also contribute to the overall plastic waste and are grouped into group 2. These plastics are acrylic, nylon, POM (Acetal), ABS, and PTFE. Table 1 lists all of these plastics, their associated commercial acronyms, their RIC, and their common end use application examples. While most plastics were collected using the RIC, others were directly purchased to guarantee the identity of the plastic resin. From each object a small sample was trimmed (to fit in the spectrometer sample holder) and cleaned to remove residues. They were labeled and sorted as per their plastic resin constituent.

The reflectance spectra were acquired using a microscope-coupled FTIR spectrometer (Hyperion 1000-Vertex 80, Bruker Optics, Inc.). The NIR reflectance spectra were measured using a tungsten filament source in combination with calcium fluoride beam splitter. The MIR reflectance spectra were measured with a glow bar thermal source paired with a potassium bromide beam splitter. In both configurations a nitrogen cooled mercury cadmium telluride (MCT) detector and a 0.4 NA Cassegrain objective lens were used. The background reference was taken with respect to a gold mirror. The spectrometer spectral resolution was 4 cm^{-1}, and the reflectance spectra were averaged 128 times. Such spectrometer resolution maps to wavelength resolution ($\Delta\lambda = \lambda^2\Delta\nu$, where λ is the wavelength of interest, $\Delta\nu$ is the spectrometer resolution in wavenumbers, and $\Delta\lambda$ is the corresponding resolution in wavelength) of 0.04 nm at 1 μm, 10 nm at 5 μm, and 40 nm at 10 μm, which are enough to resolve such broad vibrational resonances.

The reflectance of all plastic samples was collected to identify the dominant spectral features in both the NIR and MIR domains. An example of the spectral feature selection process is shown in Fig. 1, which depicts the reflectance spectra for a PET film in the NIR (Fig. 1(a)) and the MIR (Fig. 1(b)) domains, indicating the selected dominant spectral features. Two measurements per sample were taken. The spectral library containing mean spectral feature values of peaks and valleys

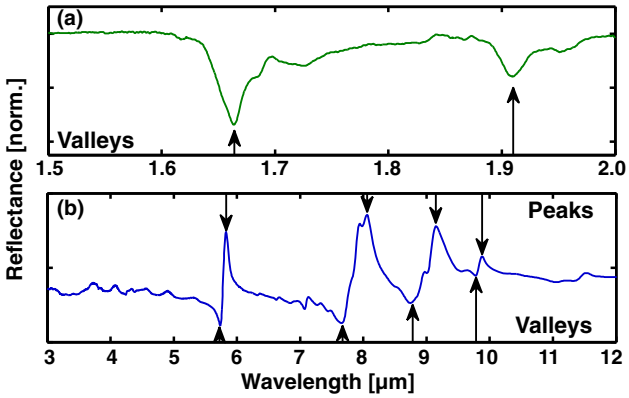

Fig. 1. Two reflectance spectra examples for PET that show how the unique spectral features are selected, in (a) NIR and (b) MIR, to construct the spectral fingerprint library.

($\lambda_{p,v}$) with its standard deviation (σ) of all plastics resin families is constructed. Finally, this library is used for database search for the blind detection of unknown plastic samples.

3. RESULTS

A. Near Infrared

The reflectance spectra were measured for both group 1 and group 2 in the NIR domain. Representative spectra for group 1 (NIR active) are shown in Fig. 2(a) (see Figs. 8–15 for more details). The spectral features are determined by the local minima (valleys) in the reflectance spectra that are tabulated in Table 2. Figure 2(b) (see Figs. 16–20 for more details) shows representative NIR reflectance spectra of plastics contained in group 2 (NIR inactive) showing a constant reflectance without any spectral feature that further vindicates the need for a multispectral and multi-dimensional detection approach.

Moreover, the addition of colorants to the base plastic matrix further complicates the detection process. The colorant present in the plastic resin matrix influences, to some extent, the NIR spectra, especially black. In Fig. 3(a) four representative spectra of HDPE for black, clear, white, and yellow samples are plotted (actual samples are shown in the inset). In Fig. 3(c) the representative spectra of red, clear, blue, and black PS samples (in solid phase) are plotted (actual samples are shown in the inset). All colored HDPE and PS (solid phase) samples have the same spectra, but only the black colored sample lacks NIR activity. In Fig. 3(b) four LDPE samples of blue, red, clear, and yellow color are plotted (actual samples are shown in the inset) showing no color variation in the NIR spectra. Colored samples of acrylic samples, on the other hand, are NIR inactive, but the clear sample is NIR active as can be observed in Fig. 3(d) (actual samples are shown in the inset).

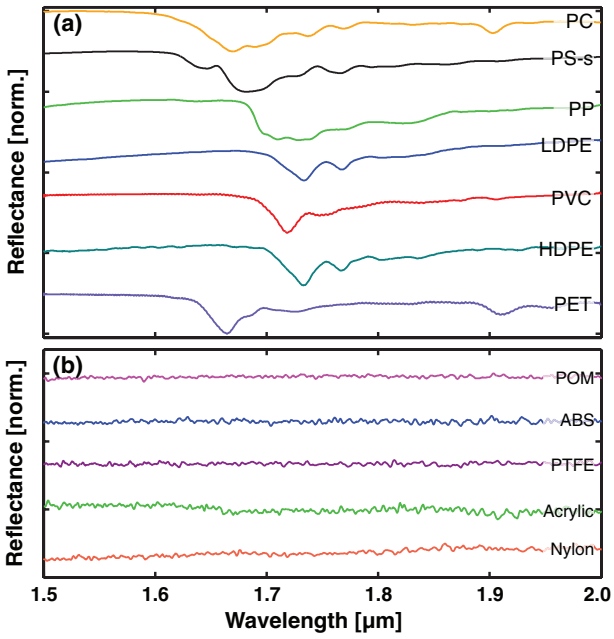

Fig. 2. Normalized NIR reflectance spectra for plastics in (a) group 1 (see Figs. 8–15 and (b) group 2 (see Figs. 16–20) for more details.

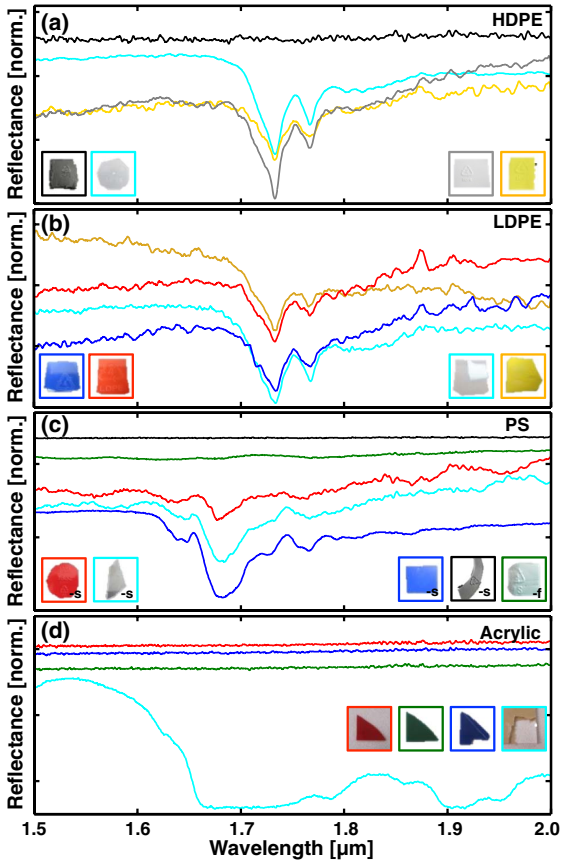

Fig. 3. NIR reflectance of several colored samples with the actual samples in the insets. (a) Black, clear, white, and yellow HDPE samples. (b) Blue, red, clear, and yellow LDPE samples. (c) Red, clear, blue, and black colored samples of PS in solid phase (-s) and green colored PS in foam phase (-f). (d) Red, green, blue, and clear acrylic samples.

Other factors that influence the quality of the samples include the surface roughness. From all samples characterized, those having considerable surface roughness displayed very weak reflectance with very shallow resonances almost buried into the noise level. Furthermore, the sample morphology such as PS in solid and foam phases affects the NIR spectra. While solid PS samples (marked as -s) display a distinctive set of spectral features, PS in foam phase (marked as -f) does not show any whatsoever; see Fig. 3(c).

From this analysis we can observe that the NIR spectroscopy alone is not sufficient for the detection of the complete set of commonly used and specialized plastics with or without color additives.

B. Mid-Infrared

The same spectroscopic measurements are performed for both groups in the MIR spectral band. Representative reflectance spectra for groups 1 and 2 are plotted in Figs. 4(a) and 4(b), respectively (see Figs. 8–20 for more details). We can observe multiple spectral features in the MIR domain for plastics in group 2, which are NIR inactive. Plastics in group 1 also demonstrate distinct spectral features in the MIR domain

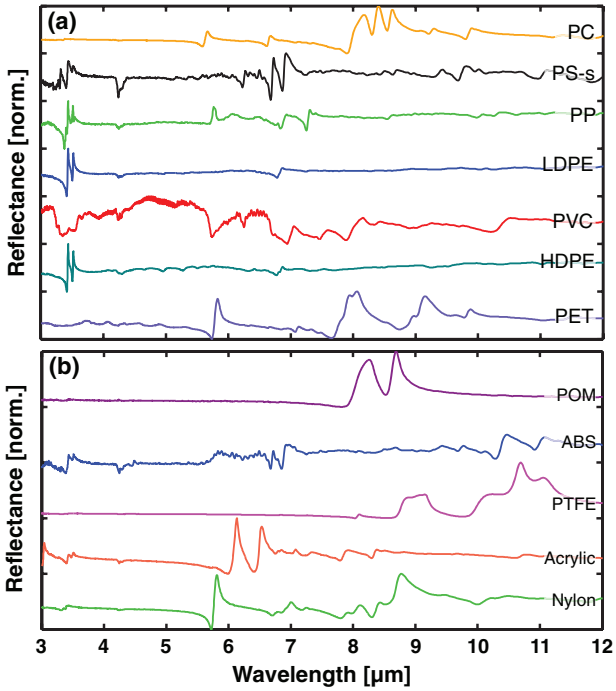

Fig. 4. MIR reflectance spectra for plastics in (a) group 1 (see Figs. 1–13 for more details).

[Fig. 4(a)] that can complement their NIR spectral signatures Fig. [2(a)].

In the NIR domain the two phases of PS (solid and foam) could not be characterized because solid phase PS samples have spectral features but not their foam phase counterparts. However, in the MIR domain both PS phases could be fully characterized but not at the exact resonance features as seen Fig. 5. The spectral features fo8r PS in foam are redshifted compared to PS in solid phase.

In addition, color does not show significant influence in the reflectance spectra; even black samples can be fully characterized in the MIR domain contrary to the NIR domain. For example, in Fig. 6(a), four spectra of colored samples of HDPE are plotted (actual samples are shown in the inset). In that graph we can observe no difference in the spectra for clear,

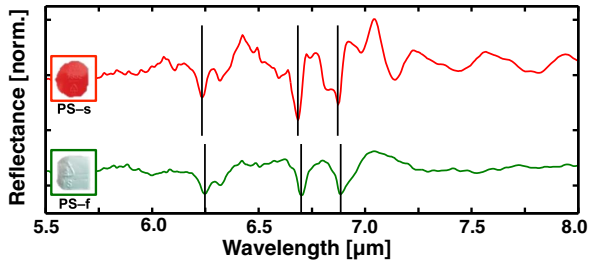

Fig. 5. Reflectance spectra of two representative PS samples in solid and foam phase. For clarity only the valleys are shown. In these morphology-dependent spectra, the spectral features (valleys represented by the vertical lines) of PS in foam phase are redshifted with respect to those of PS in solid phase.

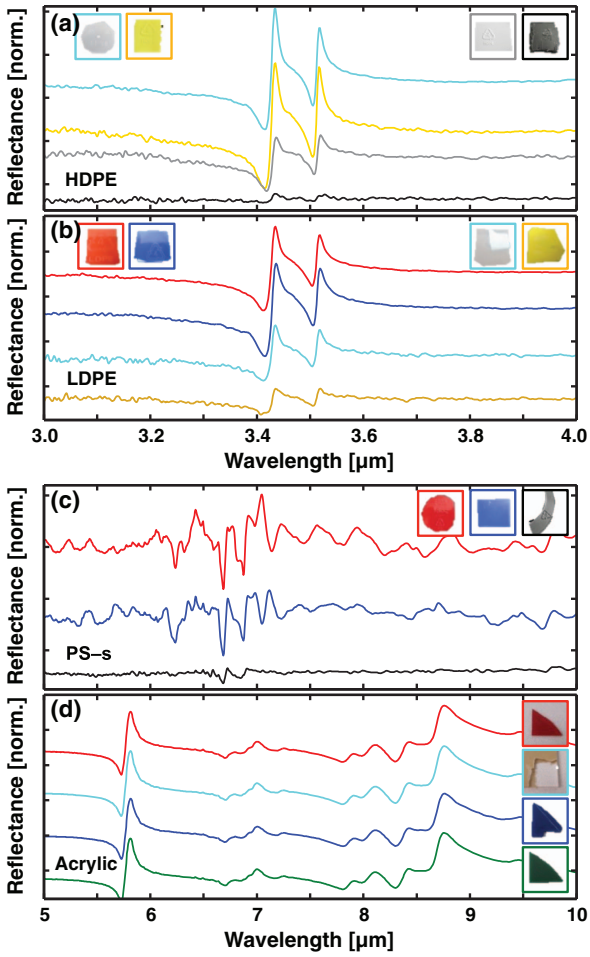

Fig. 6. MIR reflectance spectra colored samples. (a) Black, white, yellow, and clear colors of HDPE. (b) Yellow, clear, blue, and red colors of LDPE. (c) Red, blue, and black colors of PS in solid phase. (d) Red, clear, blue, and green colors of acrylic.

yellow, white, and black colored samples. The relative changes in spectral amplitude originate from the sample surface morphology. The same can be observed in Fig. 6(c) for black, red, and blue colors of solid PS samples (actual samples are shown in the inset). In Fig. 6(b), yellow, clear, blue, and red colored samples of LDPE are plotted (actual samples are shown in the inset), having the same color independency spectra. Finally, acrylic samples that had two different NIR spectra, one for colored samples (NIR inactive) and one for a clear sample (see Fig. 3(d)), are spectrally the same in the MIR domain as seen in Fig. 6(d) (actual samples are shown in the inset).

From the full collection of plastics characterized, each plastic resin family had its own set of reflectance features. Due to the diversity in morphology, surface roughness, and thickness among a specific resin family, not all spectra displayed the same spectral features, because of either low reflectance (resonances into the noise level) or no resonances present (resonances associated with specific sample constituent such as fillers). Nevertheless, a set of unique spectral features is present in each plastic resin group. From those features, selected as specified in

Table 2. Spectral Fingerprint of the 12 Plastic Resin Groups in the NIR and MIR[a]

	Plastic	Valley Wavelengths $\lambda_v(\sigma)$ [μm]							Peak Wavelengths $\lambda_p(\sigma)$ [μm]			
		NIR		MIR					MIR			
		λ_{v1}	λ_{v2}	λ_{v3}	λ_{v4}	λ_{v5}	λ_{v6}	λ_{v7}	λ_{p1}	λ_{p2}	λ_{p3}	λ_{p4}
Group 1	PET	1.664	1.910	5.739	7.67	8.764	9.769	–	5.831	8.05	9.139	9.865
		(0.000)	(0.001)	(0.002)	(0.017)	(0.02)	(0.011)	–	(0.003)	(0.013)	(0.014)	(0.007)
	HDPE	1.733	1.767	3.415	3.506	6.782	–	–	3.435	3.517	6.863	–
		(0.001)	(0.000)	(0.001)	(0.001)	(0.002)	–	–	(0.001)	(0.001)	(0.003)	–
	PVC	1.718	1.746	6.95	7.467	7.883	–	–	7.062	7.602	8.16	–
		(0.001)	(0.003)	(0.003)	(0.006)	(0.007)	–	–	(0.024)	(0.013)	(0.004)	–
	LDPE	1.733	1.767	3.412	3.505	6.786	–	–	3.435	3.519	6.864	–
		(0.002)	(0.002)	(0.002)	(0.001)	(0.003)	–	–	(0.000)	(0.000)	(0.005)	–
	PP	1.709	1.727	6.822	7.248	–	–	–	6.923	7.297	–	–
		(0.001)	(0.002)	(0.008)	(0.007)	–	–	–	(0.006)	(0.004)	–	–
	PS-s	1.682	–	3.301	3.405	6.232	6.685	6.871	3.316	3.439	6.724	6.917
		(0.002)	–	(0.003)	(0.003)	(0.002)	(0.003)	(0.007)	(0.002)	(0.006)	(0.000)	(0.004)
	PS-f	–	–	3.307	3.418	6.248	6.699	6.885	3.353	3.482	–	–
		–	–	(0.001)	(0.004)	(0.002)	(0.003)	(0.000)	(0.003)	(0.003)	–	–
	PC	1.670	1.903	7.906	8.301	8.547	–	–	8.174	8.409	8.624	–
		(0.001)	(0.001)	(0.003)	(0.000)	(0.000)	–	–	(0.004)	(0.000)	(0.004)	–
Group 2	Acrylic	–	–	5.727	7.811	8.301	–	–	5.814	7.002	8.111	8.762
		–	–	(0.003)	(0.003)	(0.000)	–	–	(0.002)	(0.000)	(0.000)	(0.005)
	POM	–	–	8.036	9.766	–	–	–	8.094	9.161	10.693	11.073
		–	–	(0.000)	(0.019)	–	–	–	(0.000)	(0.000)	(0.012)	(0.012)
	Nylon	–	–	5.995	6.378	–	–	–	6.122	6.524	–	–
		–	–	(0.008)	(0.03)	–	–	–	(0.009)	(0.01)	–	–
	ABS	–	–	6.677	6.859	10.287	10.93	–	6.721	10.463	11.083	–
		–	–	(0.007)	(0.009)	(0.006)	(0.010)	–	(0.006)	(0.012)	(0.006)	–
	PTFE	–	–	8.517	–	–	–	–	8.252	8.689	–	–
		–	–	(0.006)	–	–	–	–	(0.008)	(0.003)	–	–

[a]Peaks and valleys are separated for ease of comparison.

Fig. 1, each line with its corresponding standard deviation ($\lambda_{p,v}(\sigma)$) is tabulated in Table 2 for both the NIR and MIR domains. At least one pair of spectral lines is unique among the 12 sets of plastics that can be used to identify an unknown plastic based on this multi-spectral spectroscopy method. In addition, due to the lack of NIR spectral features for most plastics, it is not practical to incorporate this domain in an actual detection system since the MIR is proved to be sufficient to differentiate any of the 12 plastic resins characterized herein.

One limitation encountered in this method is that HDPE and LDPE cannot be differentiated since their MIR and NIR spectral features are practically the same. In the next section a blind identification of randomly selected samples from the characterized plastic batch and different plastic objects was carried out to test the validity of the method. Notice that objects matching HDPE or LDPE are identified by polyethylene (PE).

C. Blind Detection

We performed two sets of blind detection experiments of unknown plastics. The first experiment intends to validate the multi-spectral library to identify plastic resins used to construct it. From the collected set of characterized plastics 12 samples were picked up randomly. They were cut and subject to no surface treatment, such as cleaning. The reflectance spectra were recorded for each sample, and their MIR spectral features were compared to the library. A successful identification is achieved when the spectral features match with all the multi-spectral library lines of a specific resin within the range of the corresponding standard deviation. All samples were successfully identified. Figure 7(a) shows the selected plastic samples and the identified resin. The second experiment aimed to validate the multi-spectral library to identify unknown plastic objects. In total 25 objects were tested; see Fig. 7(b). We recorded the reflectance spectra and compared them to the MIR spectral features in the library. From the collection 22/25 objects were identified based on the spectral library with high confidence: spectral features falling within the acceptable standard deviation range. Due to the lack of HDPE and LDPE spectral distinction we use PE to refer to any of its two variations. Two objects, corresponding to the USB key and the salsa cup, were identified as acrylic and PS, respectively, but with low confidence since only half of the spectral features of the sample matched. One object, the power cord, was not identified because its spectral features did not match to the fingerprint of any resin in the library. The power cord is primary made of PVC according to the manufacturer's specifications; however, the presence of fillers in the polymer matrix can modify the spectral response and provided null identification due to the absence of filler material information in the present test library. A modified library that also includes the information various commercial filler materials have in the polymer matrix is needed for such composite plastic identification.

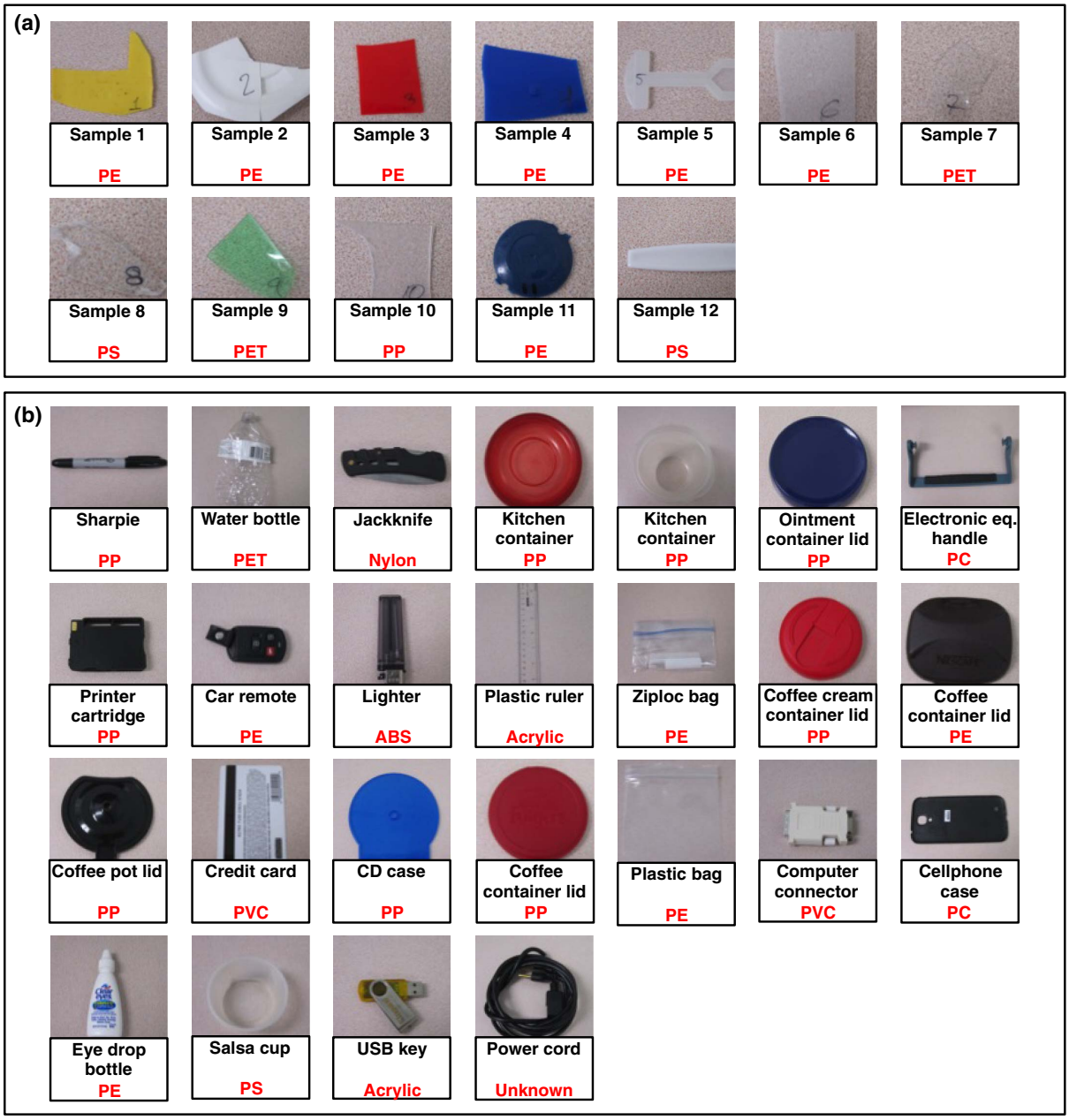

Fig. 7. Plastic samples randomly selected for the blind identification experiment based on the reported multi-spectral library. (a) Samples randomly picked from the characterized plastic batch used in experiment 1. (b) Plastic objects used in experiment 2.

4. CONCLUSIONS

Twelve plastic resin groups, which are commonly encountered in municipal waste worldwide, are characterized with FTIR reflectance spectroscopy. Based on the NIR and MIR reflectance we statistically identified the unique spectral features to construct a multi-spectral library covering the IR activity of the characterized plastic resins. Plastics in group 1 are NIR active, but not those in group 2. Furthermore, in the NIR domain there is considerable variation in the reflectance spectra among individuals of the same resin but different colors and morphology, such as the solid and foam phase of PS, the difference in spectra of colored versus clear acrylic, or the lack of spectral features in black samples. Hence the NIR domain, by itself, renders useless for blind identification of samples of the whole resin collection. In the MIR, all plastic resins can be fully characterized including the NIR inactive, those with color, or those that are morphology dependent. The selected spectral features based on peaks and valleys in the reflection spectra add an extra degree of freedom to the identification process. For practical reasons the MIR domain (from 3–12 μm) is enough to identify the whole set of resins as proved in the two blind identification experiments. The only limitation encountered is that LDPE and HDPE cannot be differentiated since their spectral features are the same in both the NIR and MIR domains.

APPENDIX A:

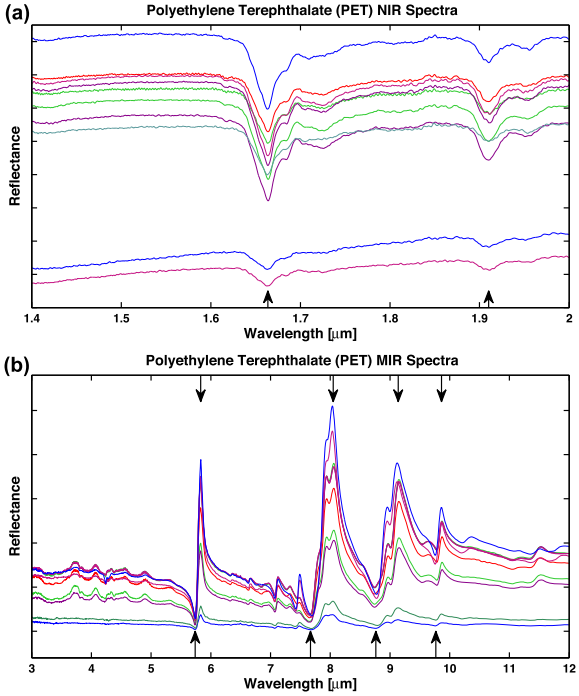

Fig. 8. Reflectance spectra of all polyethylene terephthalate (PET) samples characterized in the (a) NIR and (b) MIR spectral domains. The arrows represent the selected spectral lines, peaks and valleys, used to construct the spectral fingerprint library (Table 2).

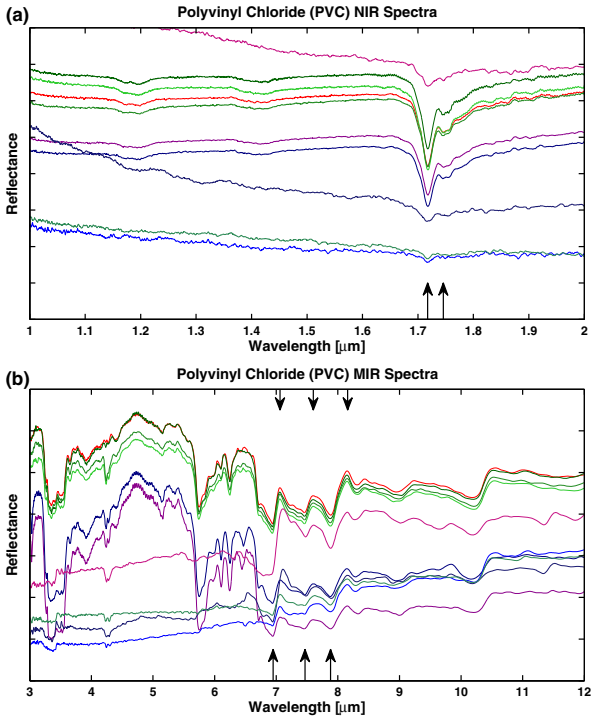

Fig. 10. Reflectance spectra of all polyvinyl chloride (PVC) samples characterized in the (a) NIR and (b) MIR spectral domains. The arrows represent the selected spectral line, peaks and valleys, used to construct the spectral fingerprint library (Table 2).

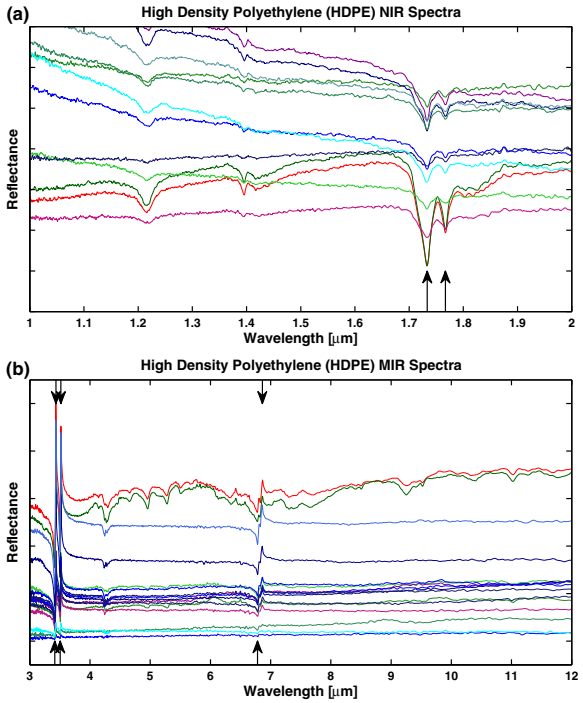

Fig. 9. Reflectance spectra of all high density polyethylene (HDPE) samples characterized in the (a) NIR and (b) MIR spectral domains. The arrows represent the selected spectral line, peaks and valleys, used to construct the spectral fingerprint library (Table 2).

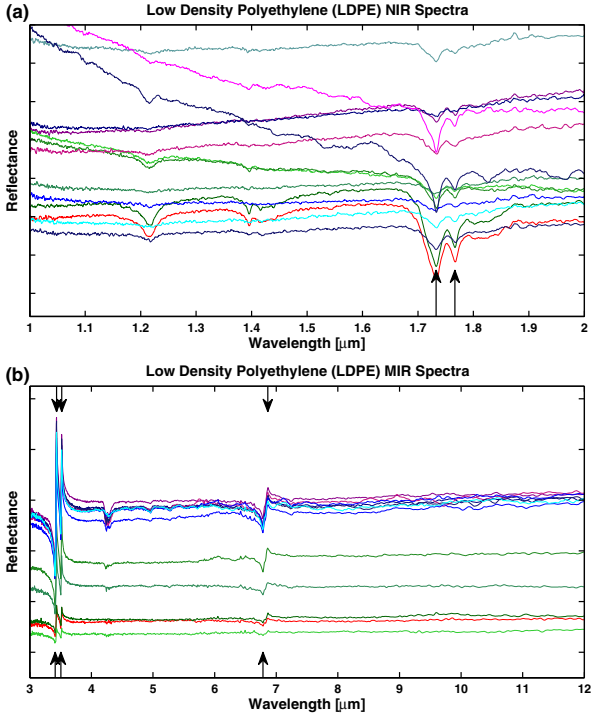

Fig. 11. Reflectance spectra of all low density polyethylene (LDPE) samples characterized in the (a) NIR and (b) MIR spectral domains. The arrows represent the selected spectral line, peaks and valleys, used to construct the spectral fingerprint library (Table 2).

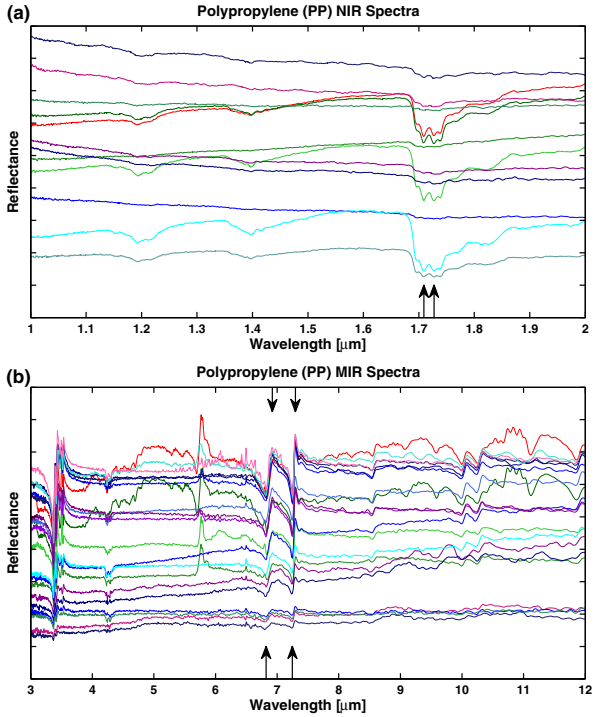

Fig. 12. Reflectance spectra of all polypropylene (PP) samples characterized in the (a) NIR and (b) MIR spectral domains. The arrows represent the selected spectral line, peaks and valleys, used to construct the spectral fingerprint library (Table 2).

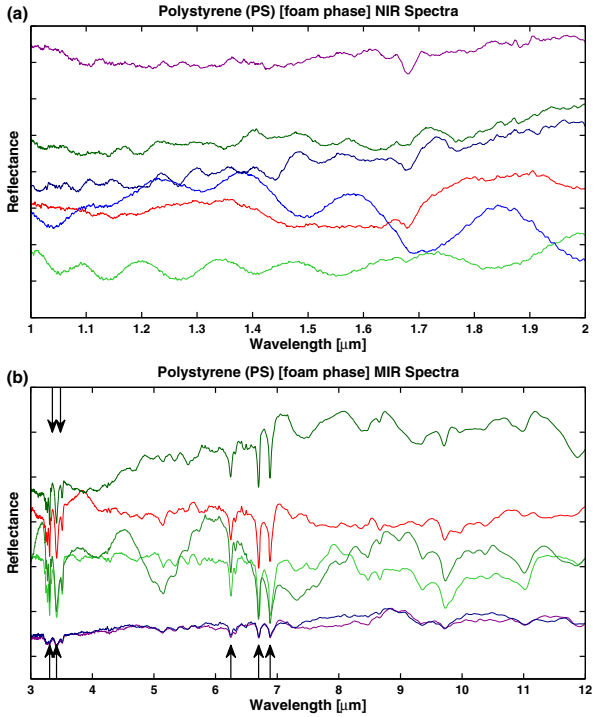

Fig. 14. Reflectance spectra of all polystyrene in foam phase (PS-f) samples characterized in the (a) NIR and (b) MIR spectral domains. The arrows represent the selected spectral line, peaks and valleys, used to construct the spectral fingerprint library (Table 2).

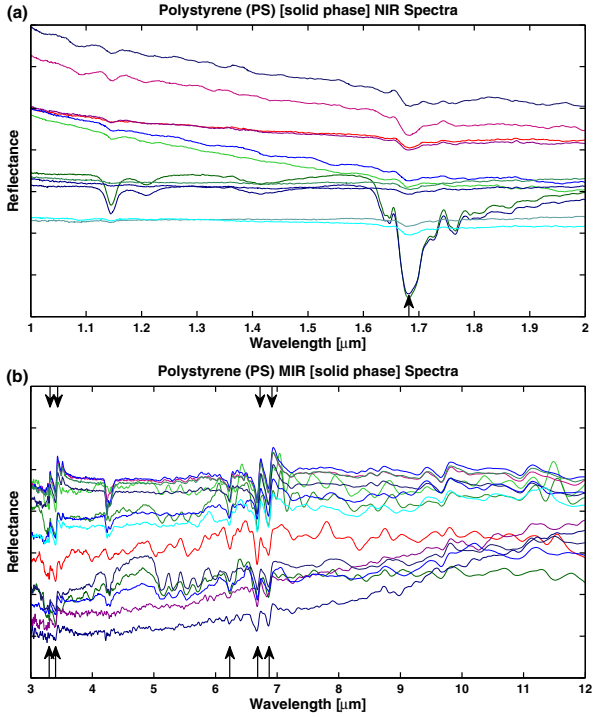

Fig. 13. Reflectance spectra of all polystyrene in solid phase (PS-s) samples characterized in the (a) NIR and (b) MIR spectral domains. The arrows represent the selected spectral line, peaks and valleys, used to construct the spectral fingerprint library (Table 2).

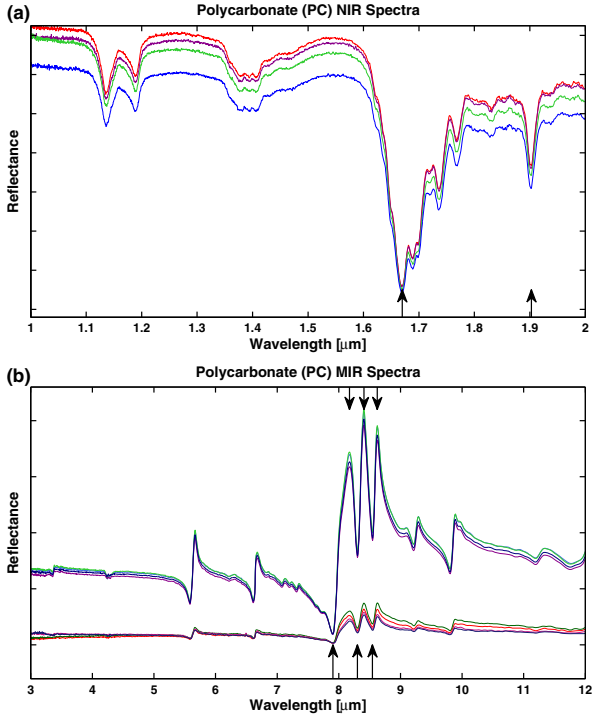

Fig. 15. Reflectance spectra of all polycarbonate (PC) samples characterized in the (a) NIR and (b) MIR spectral domains. The arrows represent the selected spectral line, peaks and valleys, used to construct the spectral fingerprint library (Table 2).

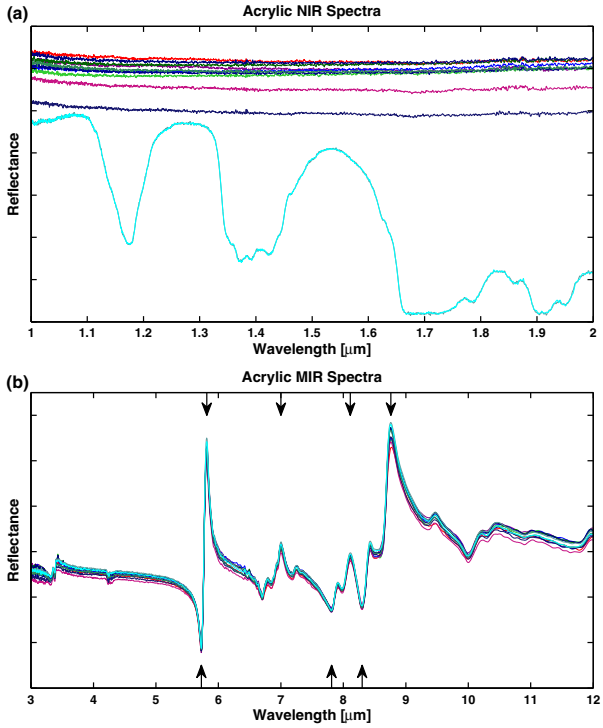

Fig. 16. Reflectance spectra of all acrylic samples characterized in the (a) NIR and (b) MIR spectral domains. The arrows represent the selected spectral line, peaks and valleys, used to construct the spectral fingerprint library (Table 2).

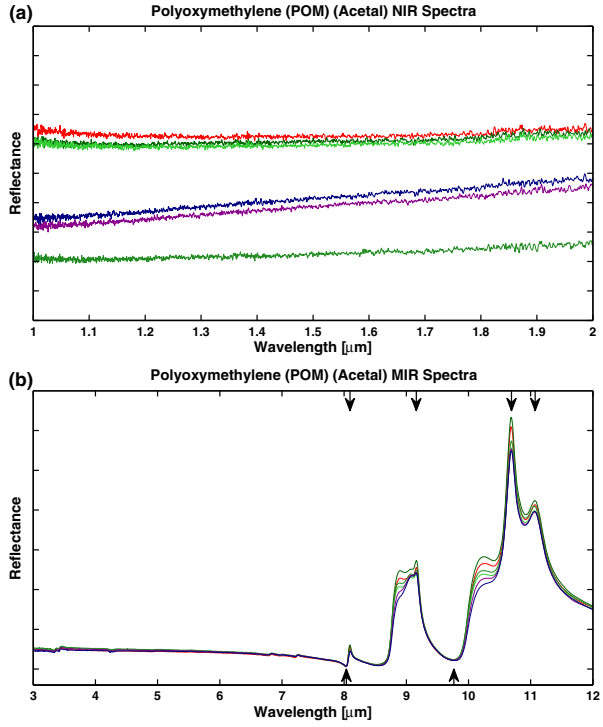

Fig. 18. Reflectance spectra of all polyoxymethylene (POM) (Acetal) samples characterized in the (a) NIR and (b) MIR spectral domains. The arrows represent the selected spectral line, peaks and valleys, used to construct the spectral fingerprint library (Table 2).

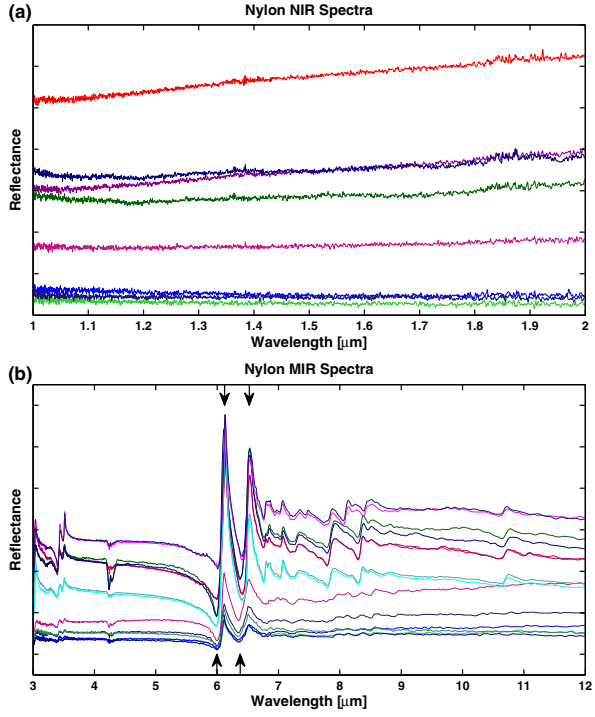

Fig. 17. Reflectance spectra of all nylon samples characterized in the (a) NIR and (b) MIR spectral domains. The arrows represent the selected spectral line, peaks and valleys, used to construct the spectral fingerprint library (Table 2).

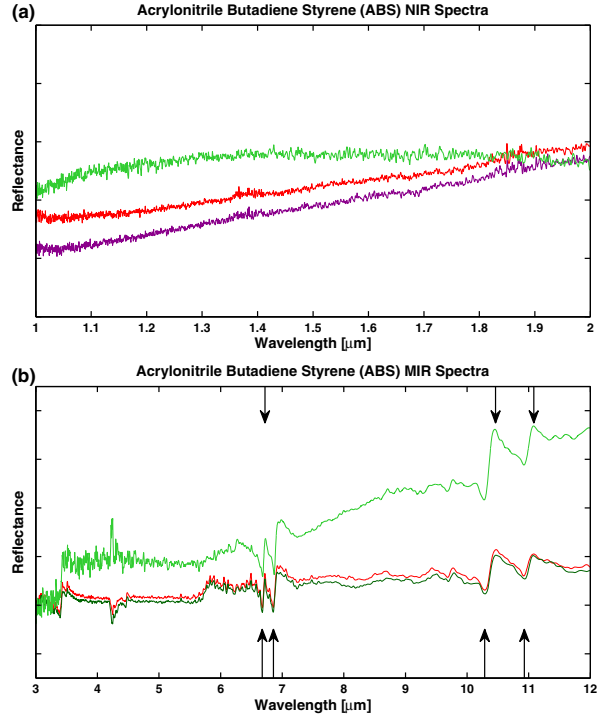

Fig. 19. Reflectance spectra of all acrylonitrile butadiene styrene (ABS samples characterized in the (a) NIR and (b) MIR spectral domains. The arrows represent the selected spectral line, peaks and valleys, used to construct the spectral fingerprint library (Table 2).

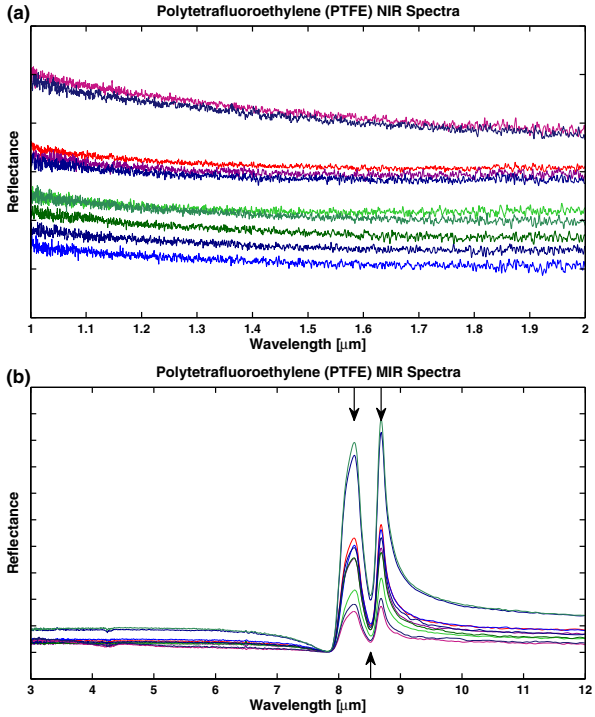

Fig. 20. Reflectance spectra of all polytetrafluoroethylene (PTFE) samples characterized in the (a) NIR and (b) MIR spectral domains. The arrows represent the selected spectral line, peaks and valleys, used to construct the spectral fingerprint library (Table 2).

Funding. Florida Space Institute (FSI)/NASA (63019022); National Council of Science and Technology (Consejo Nacional de Ciencia y Tecnología—CONACyT).

REFERENCES

1. P. M. Subramanian, "Plastics recycling and waste management in the US," Resour. Conserv. Recycl. **28**, 253–263 (2000).
2. USEPA, Municipal solid waste generation, recycling, and disposal in the united states: facts and figures for 2012 (2014), http://www.epa.gov/solidwaste/nonhaz/municipal/msw99.htm.
3. H. Shent, R. J. Pugh, and E. Forssberg, "A review of plastics waste recycling and the flotation of plastics," Resour. Conserv. Recycl. **25**, 85–109 (1999).
4. J. Hopewell, R. Dvorak, and E. A. Kosior, "Plastics recycling: challenges and opportunities," Philos. Trans. R. Soc. B **364**, 2115–2126 (2009).
5. G. Wu, J. Li, and Z. Xu, "Triboelectrostatic separation for granular plastic waste recycling: a review," Waste Management **33**, 585–597 (2013).
6. G. Dodbiba, A. Shibayama, J. Sadaki, and T. Fujita, "Combination of triboelectrostatic separation and air tabling for sorting plastics from a multi-component plastic mixture," Mater. Trans. **44**, 2427–2435 (2003).
7. H.-S. Jeon, C.-H. Park, B.-G. Cho, and J.-K. Park, "Separation of PVC and rubber from covering plastics in communication cable scrap by tribo-charging," Sep. Sci. Technol. **44**, 190–202 (2009).
8. S. Serranti, V. Luciani, G. Bonifazi, B. Hu, and P. C. Rem, "An innovative recycling process to obtain pure polyethylene and polypropylene from household waste," Waste Management **35**, 12–20 (2015).
9. E. J. Bakker, P. Rem, A. J. Berkhout, and L. Hartmann, "Turning magnetic density separation into green business using the cyclic innovation model," Open Waste Manage. J. **3**, 99–116 (2010).
10. H. Wang, X.-L. Chen, Y. Bai, C. Guo, and L. Zhang, "Application of dissolved air flotation on separation of waste plastics ABS and PS," Waste Management **32**, 1297–1305 (2012).
11. E. Scavino, D. A. Wahab, A. Hussain, H. Basri, and M. M. Mustafa, "Application of automated image analysis to the identification and extraction of recyclable plastic bottles," J. Zhejiang Univ. Sci. A **10**, 794–799 (2009).
12. G. Dodbiba and T. Fujita, "Progress in separating plastic materials for recycling," Phys. Sep. Sci. Eng. **13**, 165–182 (2004).
13. G. Dodbiba, J. Sadaki, and A. Shibayana, "Sorting techniques for plastics recycling," Chin. J. Process Eng. **6**, 186–191 (2006).
14. H. Masoumi, S. M. Safavi, and Z. Khani, "Identification and classification of plastic resins using near infrared reflectance spectroscopy," World Acad. Sci. Eng. Technol. **6**, 141–148 (2012).
15. J. F. Masson, L. Pelletier, and P. Collins, "Rapid FTIR method for quantification of styrene-butadiene type copolymers in bitumen," J. Appl. Polym. Sci. **79**, 1034–1041 (2001).
16. V. Allen, J. H. Kalivas, and R. G. Rodriguez, "Post-consumer plastic identification using Raman spectroscopy," Appl. Spectrosc. **53**, 672–681 (1999).
17. S. Barbier, S. Perrier, P. Freyermuth, D. Perrin, B. Gallard, and N. Gilon, "Plastic identification based on molecular and elemental information from laser induced breakdown spectra: a comparison of plasma conditions in view of efficient sorting," Spectrochim. Acta B **88**, 167–173 (2013).
18. J. Anzano, R.-J. Lasheras, B. Bonilla, and J. Casas, "Classification of polymers by determining of C1:C2:CN:H:N:O ratios by laser-induced plasma spectroscopy (LIPS)," Polym. Test. **27**, 705–710 (2008).
19. A. Ulrici, S. Serranti, C. Ferrari, D. Cesare, G. Foca, and G. Bonifazi, "Efficient chemometric strategies for PET–PLA discrimination in recycling plants using hyperspectral imaging," Chemom. Intell. Lab. Syst. **122**, 31–39 (2013).
20. S. Serranti, A. Gargiulo, and G. Bonifazi, "Hyperspectral imaging for process and quality control in recycling plants of polyolefin flakes," J. Near Infrared Spectrosc. **20**, 573–581 (2012).
21. J. M. Chalmers and P. R. Griffiths, *Handbook of Vibrational Spectroscopy* Vol. **3**: Sample Characterization and Spectral Data Processing (Wiley, 2002).
22. V. Lucarini, J. J. Saarinen, K. E. Peiponen, and E. M. Vartiainen, *Kramers-Kronig Relations in Optical Materials Research* (Springer-Verlag, 2005).
23. M. Claybourn, P. Colombel, and J. Chalmers, "Characterization of carbon-filled polymers by specular reflectance," Appl. Spectrosc. **45**, 279–286 (1991).